

Pressure Solution Mass Transfer of the Purgatory Conglomerate

Thomas P. Winger

Adviser: Mark Brandon

Additional Readers: Danny Rye

May 1st, 2013

A Senior Thesis presented to the faculty of the Department of Geology & Geophysics, Yale University, in partial fulfillment of the Bachelor's Degree.

In presenting this thesis in partial fulfillment of the Bachelor's Degree from the Department of Geology and Geophysics, Yale University, I agree that the department may make copies or post it on the departmental website so that others may better understand the undergraduate research of the department. I further agree that extensive copying of this thesis is allowable only for scholarly purposes. It is understood, however, that any copying or publication of this thesis for commercial purposes or financial gains is not allowed without my written consent.

Thomas Patrick Winger, 01 May, 2013

Abstract

Pressure solution is believed to have significantly deformed the clasts of the Purgatory Conglomerate. The Pennsylvanian quartzite conglomerate is exposed throughout the southern Narragansett Basin of Rhode Island and was subject to normal Barrovian-type metamorphism during the suture-rift tectonics of the Alleghanian Orogeny. Field observation indicates the conglomerate has experienced significant volume loss deformation by pressure solution on the order of 50-90%, with no local sink for the solved material. If correct, this volume strain data indicates a large quantity of fluid must have passed through the conglomerate with the capacity to dissolve and transport a significant amount of material out of the system. This process is called solution mass transfer (SMT).

Volume strain calculations have been made for 11 outcrops across southern Rhode Island using R_f/Φ analysis on clasts from oriented photographs of the Purgatory Conglomerate to produce representative 3D strain ellipsoids. Corresponding measurements of the modal abundance of fibrous overgrowth support advective transport of material away from the source clasts and out of the conglomerate unit. It has been shown that clast interiors remain undeformed with very thin micaceous selvages having formed at clast margins, a product of pressure solution mass transport. Weathering rims visible within cobble margins and metamorphic overprinting of the conglomerate help constrain the deformation history and may offer new insight into the sequence of pressure solution events in the Purgatory Conglomerate.

Included is a discussion of the source and nature of the fluid active in the pressure solution mass transfer deformation of the Purgatory Conglomerate. Intrusion of Permian granite to the southwest of the conglomerate is a possible source of the metamorphic gradient, however a reported increase in metamorphic gradient eastward from chlorite to biotite subfacies of the greenschist facies might suggest a more complex metamorphic reconstruction. Furthermore, the conglomerate layer is in stratigraphic sequence with Carboniferous sandstone and coaly shale layers, providing conditions for a fluid with high solute activity. A model for oxygen isotope exchange between the Purgatory Conglomerate and the fluid phase active during pressure solution is presented.

Contents

Introduction	4
Background to Pressure Solution Mass Transfer	5
Study Area	12
Stratigraphy of the Study Area	12
Tectonic History	15
Evidence for Pressure Solution	17
Study Sites	21
Methods	23
Shape analysis	23
Modal abundance of fibrous overgrowth	24
Volume loss	25
Fold axis	25
Results	26
Discussion	26
Regional Variation in Volume Loss and Ellipsoid Geometry	- 26
Fluid Physiochemistry	33
Conclusions	37
Acknowledgements	38
Works Cited	38
Appendix	42

Introduction

Pressure solution has long been recognized as an important deformation mechanism in rock rheology, diagenesis, and metamorphism (e.g., Sorby 1863, 1865; Adams & Coker 1910; Tada and Siever, 1989). The term “Pressure Solution” comes from the presence of a fluid film along grain-grain contacts during deformation that acts as a vessel for solute transport during non-penetrative ductile deformation (Weyl, 1958, 1959). In geological systems the identification of mass loss during pressure solution deformation has led to the use of the term “Solution Mass Transfer” (SMT) for the process (Brandon 1994; Ring & Brandon 1999). The mechanisms that control the onset of SMT during pressure solution remain unclear, posing unique problems for geologists and engineers alike. Furthermore the theory of solution mass transfer and its role in geological systems remains debated, as many rocks are recognized as having undergone constant-volume pressure solution deformation.

The Purgatory Conglomerate of southern Rhode Island is known to have undergone extensive pressure solution (e.g., Mosher 1976, 1978; McPherrren and Kuiper 2013) resulting in oriented clasts with geometries that vary regionally. Upon further inspection the clasts – which vary in size from pebble to boulder – appear to have experienced tremendous non-penetrative volume loss deformation, providing us the ideal natural laboratory to study SMT. The clasts of the conglomerate are mostly quartzite, having low solubilities under the chlorite – biotite metamorphic conditions observed. It is thus recognized that the fluid active in SMT deformation of the Purgatory Conglomerate must have evolved to transport an increasing silica solute load; perhaps travelling up-gradient in temperature or becoming more basic in pH.

The aim of this study was to calculate oriented representative 3d strain ellipsoids and volume loss estimates for 11 conglomerate outcrops. This data was then used to better understand the nature of fluid-solid interaction during SMT deformation of the Purgatory Conglomerate. The

combination of strain data and fluid determination will aid in our understanding of the tectonic formation of the Narragansett Basin and, more broadly, Pangean tectonism.

Background to Pressure Solution Mass Transfer

The first thermodynamic representation of what is today called pressure solution was developed by JW Gibbs in 1878 when he proposed the following relationship between a non-hydrostatically stressed flat solid surface and its solution (adapted here as done by Paterson 1973; Gibbs 1906):

$$(1) \quad \mu_L = u_s - TS_s + \sigma_n v_s$$

where μ_L is the chemical potential of the solute in solution; u_s , s_s are the specific internal energy and specific entropy of the stressed solid phase; T is the absolute temperature; σ_n is the normal stress to the surface of the solid; and v_s is the molar volume of the stressed solid. Equation (1) refers to a system in local equilibrium with respect to the concerned site of dissolution. Paterson (1973) notes the solubility will be independent of the fluid pressure if the state of normal stress in the solid, σ_n , is constant (assuming the activity coefficient of the solute in solution is constant). In geological systems this is rarely the case as pore fluid pressures act to weaken solid pressures from tectonic stresses. The following equation, from Paterson (1973) and Durney (1976), demonstrates the exponential relationship between solubility, $C(T, P_s, P')$, and effective pressure, $P' = P_s - P_f$:

$$(2) \quad C(T, P_s, P') = C(T, P_s, P')_0 \exp\left[\frac{v_s P'}{RT}\right]$$

where $C(T, P_s, P')_0$ is a determined solubility with $P' = 0$, an equilibrium condition with no effective pressure acting on the solid surface; v_s is the molar volume of the stressed solid; R and T are the gas constant and absolute temperature. The expected increase in solubility with increase in effective

pressure has been confirmed in many experimental studies, for example the work of Elias and Hajash (1992) or the detailed work of Fournier and Potter (1982) [Figure 1].

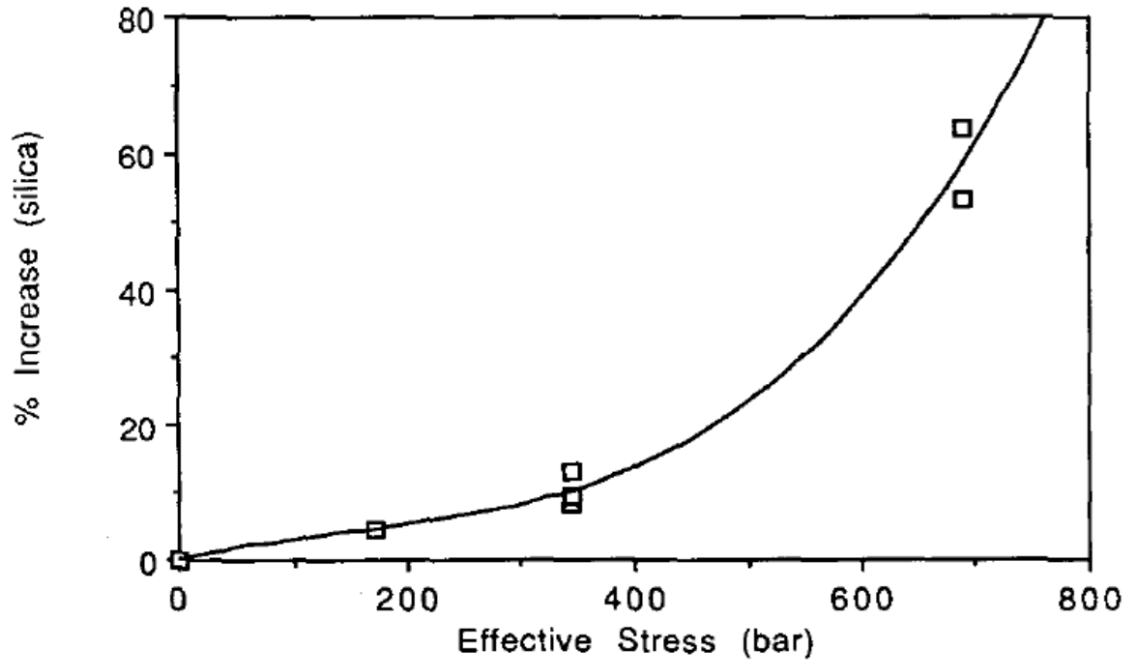


Figure 1 - Silica solubility with change in Effective Stress. From Elias and Hajash 1992

The importance of fluid along grain boundaries in pressure solution was well illustrated by PK Weyl (1958, 1959), who applied the advection-dispersion equation for solute transport in calcite and developed a pressure solution model for spheres in a cubic packing orientation that considered how fractional compaction, ζ , varies with time :

$$(3) \quad \frac{d\zeta}{dt} = 32Dmb\Sigma/(\pi a^3 \rho^3)$$

D is the diffusion constant, assumed to be constant across the fluid film; m is a film thickness constant (see Weyl 1959 for illustration); b is the stress coefficient of solubility; Σ is the effective overburden pressure; a is the radius of the spherical grain; and ρ is the radius of the contact zone.

Fractional compaction is considered a scalar quantity representing a decrease in radius of the deforming sphere in the minimum stretch direction, S_z , given an initial spherical radius of 1. Weyl describes the complete dissolution of solute at grain contacts followed by transport to regions of lower applied stress and thus lower solute chemical potential, resulting in dynamic supersaturation and precipitation of the solute (Weyl 1959). This phenomenon is pressure solution. In silica pressure solution the precipitate would be amorphous silica (De Boer *et al.* 1977) A review of pressure solution was completed in 1983 by E.H Rutter and included his previously developed constitutive flow law derived from the following three conditions (Rutter 1983):

- (a) Laplace's equation - $\nabla^2 \mu_L = 0$
- (b) A mechanical equilibrium condition dependent on interfacial geometry accounting for distribution of stress on grains from the bulk rock stress
- (c) Equation (1) relating the applied stress on a solid to its solubility

Resulting in the following strain rate equation (adapted similar to Raj & Ashby 1971):

$$(4) \quad \dot{\epsilon} = AL_{\alpha}\sigma V_{\alpha}w/d^3$$

where A is a dimensionless constant; σ is the applied uniaxial stress; w is the effective thickness of the intergranular fluid film; L_{α} is a constant that accounts for both temperature dependence and the stress-solubility relationship similar to b in equation (3); and d is grain diameter. Equation (4) is a power law relationship between strain rate and grain diameter, such that increasing grain size while holding the rest of the right hand side of (4) constant results in a decrease in strain rate. The same power law relationship ($\dot{\epsilon} \propto d^{-3}$) was calculated in the 1960's from studies of the nature and rate-limiting process in creep deformation of Al_2O_3 and is known as Coble Creep after R. L. Coble (Coble, 1963a,b,c). Coble's studies were in part a continuation of work by Nabarro & Herring who

calculated a flow law for vacancy flow creep; a penetrative deformation. The aluminum ion lattice diffusion coefficient is several orders of magnitude larger than the oxygen ion lattice diffusion coefficient, resulting in transport of oxygen along grain boundaries where the diffusion coefficient is much greater than in the crystal lattice. For grain boundary diffusion creep of Al₂O₃ Coble found:

$$(5) \quad \dot{\epsilon} = 150\sigma(D_{gb}W)/(d^3)kT$$

where D_b is the diffusion coefficient for the grain boundary layer; W is grain boundary thickness; and kT is Boltzmann's constant and absolute temperature (from Coble 1963b).

The above representations of pressure solution all consider the deformation to be *constant-volume*; that is mass is conserved and the solution to the continuity equation for a single grain is zero ($dV/dt=0$). Laboratory experiments, such as those above (Coble 1963) and others looking at pressure solution in geological systems, for example the work of De Boer *et al.* (1977) on quartz sand, observe strain of grains with length scales of μm (10^{-6}m). It is understood that application of the above pressure solution theory may need adjustment in dealing with pressure solved rocks; it is unknown if the Coble Creep power law holds for grains of considerably larger grain size ($\sim\text{cm}$). Simple inspection of the rate of strain ($\dot{\epsilon}$) must also be adjusted for solution mass transfer volume loss, as growth of the maximum principal stretch (S_x) would be less than the case of constant volume strain. It is recognized that traditional models of pressure solution are limited in their application to pressure solution mass transfer in geological settings where volume loss has occurred. This has been recognized and work has been done to develop an open-system model of pressure solution where grain boundary diffusion is accompanied by dissolution (e.g., Lehner 1995). The Lehner model for what he calls Intergranular Pressure Solution (IPS) considers the dissipation of work associated with irreversible processes in an island- channel granular contact zone, Δ , as a sum of work dissipated in dissolution of solute and work dissipated in grain boundary diffusion:

$$(6) \quad \begin{aligned} \dot{\Delta} = \dot{m} \int_{S_{gb}} [\mu_n^s(r) - \mu(r)] dA \\ + \dot{m} \int_{S_{gb}} [\mu(r) - \mu(a)] dA \end{aligned}$$

Where \dot{m} is work dissipated per unit area; $\mu_n^s(r)$ is the normal component of the solid-phase chemical potential along the solving interface; $\mu(r)$ is the chemical potential of the solute in the grain boundary fluid at the site of dissolution; $\mu(a)$ is the chemical potential of the solute at the contact periphery, or the pore space; and S_{gb} is the length of the contact interface (Lehner 1995, see [Figure 2] for an illustration of the IPS model.) Equation (6) is a clear illustration of the sequential processes in dissolution and transport of solute by grain boundary diffusion. The first integral in (6) is the rate of work dissipated in dissolution across the solid interface; The second integral is the diffusive component of the proposed IPS along grain boundaries in fluid films. Solute flux within the grain boundary from site of dissolution to pore space follows Fick's law:

$$(7) \quad J_r^{gb} = -\rho^f D_{gb} \delta dC/dr$$

where J_r^{gb} is the diffusive solute flux ($\text{kg m}^{-1} \text{s}^{-1}$) in the grain boundary; ρ^f is the density of the fluid; dC/dr is the solute concentration gradient along the direction of transport; and δ is the mean contact zone thickness. The physiochemical nature of a grain boundary fluid film is such that velocities are zero or negligible (no-slip condition) within the contact zone and thus all transport from granular contacts to pore space occurs by diffusion.

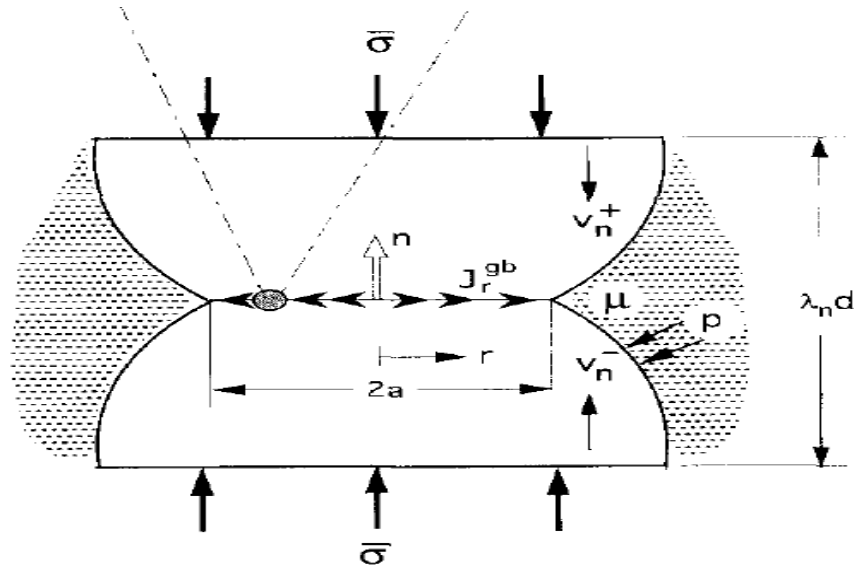


Figure 2 - Grain-grain contact during intergranular pressure solution. From Lehner 1995. J_r^{gb} denotes solute flux

There appears to be only one reasonable method for pressure solution mass transfer in geological systems to result in solute transport away from parent grains; solute must be perturbed out of the grain boundary fluid film and enter the advective pore fluid once the contact periphery has been reached. For this to occur the solute must not achieve saturation once the pore space has been reached, as was observed and discussed in the pressure solution models above (e.g., Weyl 1959). The drop in the effective stress (σ) and thus chemical potential of the solute in solution (μ) observed away from granular contacts - the driving force in precipitation- is diminished by dilution of solute concentration in the grain boundary film. This dilution is the result of solute scavenging by the pore fluid and can be modeled with Fick's law (7) where the solute concentration and velocity of the advecting pore fluid control mass transfer from the grain boundary layer to the pore fluid. Velocity is not explicitly expressed in Fick's law yet it is widely accepted that an increase in average pore fluid velocity has a 'thinning' result on the thickness of the fluid boundary layer present on the fluid-grain interface, increasing the concentration gradient between the solute load of granular

contacts and that of the associated advecting pore fluid. The nature of this physiochemical relationship as it pertains to SMT is such that an increase in average pore fluid velocity results in an increase in rate of solute transfer from the grain boundary fluid film to the advective body, and thus an increase in rate of volume loss.

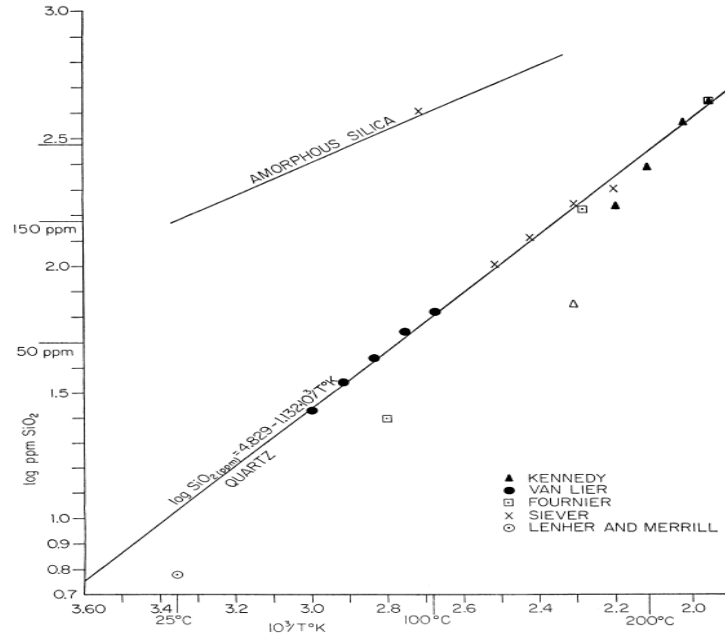


Figure 3 - Silica solubility with temperature. From Siever 1962

Other phenomena can similarly produce changes in solubility of the pore fluid. For example, silica solubility increases in aqueous solution with increased temperature T, and with increased pH (7) [Figure 3].

The above discussion of SMT as derived from general pressure solution theory provides an understanding of the physical and chemical processes involved in the mass-loss deformation mechanism. Emphasis is again placed on taking careful consideration in applying this theory to pressure solved rocks found in nature. In summary there appears to be an appreciable amount of

pressure solution theory that is not readily acceptable for application of pressure solution mass transfer to certain geological systems:

- The grain size dependence ($\dot{\epsilon} \propto d^{-3}$) for grain boundary diffusion postulated by Coble (1963) may not hold if pebble and cobble sized clasts are treated as individual deforming grains
- There is no accepted representation of the scavenging of solute from the grain boundary layer by the pore fluid; that is it is not known exactly what turns on solution mass transfer in a system experiencing pressure solution.
- The physical geometries used in thermodynamic calculation of pressure solution are not representative of what is observed in nature.

Continued study of open system pressure solution mass transfer will build on present understanding of the process.

Study Area

Stratigraphy of the Carboniferous Narragansett Basin

The Purgatory Conglomerate is exposed throughout the southern region of the Narragansett Basin in Rhode Island [Figure 4]. The conglomerate is of Pennsylvanian age (320-290 Ma) and is in stratigraphic sequence with lithic greywacke sandstone – the Rhode Island Formation – frequently seen interbedded with the conglomerate (Towe 1959; Mosher 1976).

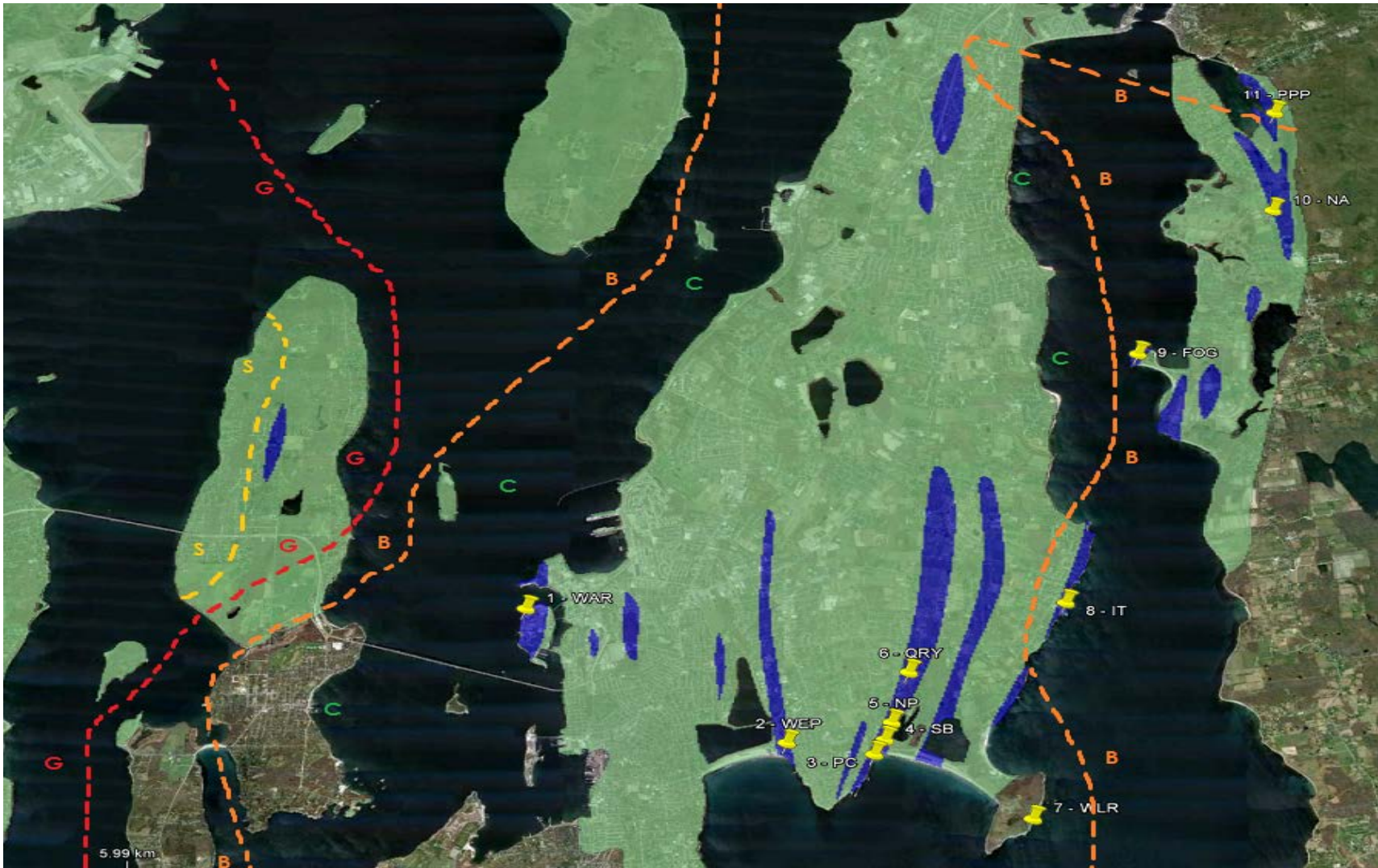


Figure 4 - Study area. Nomenclature defined in text. Light green is the Rhode Island Formation Sandstone. Dark Blue is Purgatory Conglomerate as indicated by the RI State Map North is up, East to the right

Clasts of the Purgatory Conglomerate have been classified as 95% quartzite and 5% granite, have fossil dates of late Cambrian-Ordovician age (540-440 Ma)(Walcott 1898; Towe 1959) and the unit is clast-supported; that is matrix appears to be <15% of the conglomerate by volume (Towe 1959; Mosher 1978; field observation). Clast size varies considerably from pebble (4-8 mm) to boulder (>256 mm) and appears to be dominated by cobble sized clasts (64-256mm). An accurate distribution of clast sizes in the conglomerate is absent, however field observations indicate the conglomerate is well sorted, similar to depositional features observed in fluvial systems (e.g., Posamentier, 1988). The first detailed study of the Carboniferous Narragansett Basin was published in 1899 and notes the possible relation of clast composition to the underlying lithology; i.e., conglomerate overlying granitic rock has a greater abundance of feldspathic clasts (Shaler 1899), in places becoming the dominant clast lithology. This may be seen in the many conglomerates of the Narragansett Basin and has implications for the nature and fate of basement rock during basin formation.

The Rhode Island Formation sandstone can be considered a matrix unit that interfingers four distinct stratigraphic units of the Narragansett Basin. From oldest to youngest these are (Towe 1959);

- (1) The Pondville Conglomerate – a basal conglomerate resting unconformably on underlying plutonic and metamorphic basement. Clasts are both quartzite and granitic and appear less rounded than other conglomerates in basin. Clasts are poorly sorted.
- (2) The Wamsutta Formation – a ferruginous mixture of conglomerate, sandstone, and shale, exposed at the northern extent of the Narragansett Basin. Red staining is seen as an iron oxide overprinting.

- (3) The Dighton Conglomerate – a conglomerate unit of similar geology as the Purgatory Conglomerate. Clasts are poorly sorted, are ~70% quartzite, and lack of characteristic fossils between the two layers (Dighton and Purgatory) prevent analysis of stratigraphic equivalence to the Purgatory.
- (4) The Purgatory Conglomerate – described above. It is emphasized that, unlike the underlying layers, the Purgatory is well sorted and clasts are 95% quartzite.

As mentioned all layers exhibit interbedding of Rhode Island Formation sandstone, most notably in the Dighton and Purgatory Conglomerates. Interbedded sandstone is generally lithic greywacke however is appreciably arkosic in the northern Wamsutta Formation (Towe 1959). Conglomerate outcrop to the north and west of Aquidneck Island have been documented in relation to not just Rhode Island Formation but also organic rich coaly shale layers (Shaler 1899).

Tectonic History

The Narragansett Basin formed during the suture-rift tectonics of the Alleghanian orogeny – a late event in the more general Appalachian orogeny of Pangean tectonism (e.g., Mosher 1983). The basin is a composite epi-epieugeosyncline N-S trending fold axes. Epi-epieugeosyncline structure is characterized by steep normal and thrust faulting producing deep troughs of rapid subsidence (e.g., Kay 1951; Towe 1959). The northern portion of the basin, characterized by the oxidized redbeds of the Wamsutta Formation, is believed to have been elevated with respect to the rest of the basin and thus a general topographic gradient is presumed, decreasing in elevation to the south (Towe 1959). Mosher eloquently states “Alluvial fan, braided stream, and floodplain depositional systems can be traced laterally from the uplifted margins into the lower gradient basin formed by the graben... These clastic sequences were interrupted by bimodal volcanic flows (basalts and rhyolites) and

associated lahars, an interplay of sedimentation and volcanism characteristics of continental rifting” (Mosher 1983, p. 329-330 and citations therein). The presence of organic rich coaly shale throughout the basin is representative of flood-plain development in the troughs of the synclinal basin and suggest the depositional environment was substantially wet (Shaler 1899; Mosher 1978), perhaps as an intermontane basin. Tectonic recreation by Mosher (1983) relies on significant sinistral transtensional shear for development of the mature basin. Basin formation began with early formation of a distinct northern graben and smaller graben to the south, subsequently coalescing to produce the mature Narragansett Basin. The NE trending sinistral strike-slip zone is believed to extend SW beneath Long Island (McMaster *et al.* 1980) and extending beneath Cape Cod Bay to the NE (Skehan *et al.* 1979), which would result in sinistral motion assuming E-W extension (McMaster *et al.* 1980; Mosher 1983). The source of sediment for the southern graben, including the Purgatory Conglomerate, is interpreted to be the topographic highs associated with normal faulting in the southern graben (Mosher 1983). These N-S trending normal faults are the result of sinistral strike-slip motion along the regional NE trending faults. There is no observed strike slip motion on these intrabasinal faults during deposition (Mosher 1983). A northeast trending cross section produced by Mosher attempts to illustrate the intricate folding of the deformed conglomerate [Figure 5]. It appears much of the section was based on old maps (Lahee 1912) and lack of field evidence suggests this cross section is purely schematic. Intrusion of a peraluminous, S-type granite roughly 10 km to the southwest of the present day conglomerate during the initial stage of basin formation (crystallization age=273 Ma) has produced east-west metamorphic zoning [Figure 4].

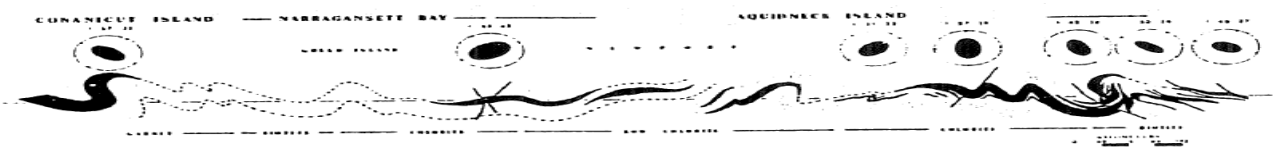


Figure 5 - Schematic cross section, from Mosher 1978. Her representative YZ sections are shown

Evidence for Pressure Solution and Solution Mass Transfer Volume Loss

Pressure solution deformation of the Purgatory Conglomerate was the focus of a PhD thesis by Sharon Mosher (1978). Inspection of the conglomerate immediately yields obvious evidence for pressure solution; clasts are rounded and smooth, indentations or ‘pits’ have developed at cobble contacts, and thin fibrous overgrowths of quartz and mica extending off the apparent long axis indicate transport of silica along clast boundaries [Figure 6a,b] (e.g., Mosher 1978; field observation). The strain shadows growing off the terminations of the major stretch axis are shown to consist of both precipitated and detrital quartz grains, composing over 75% of the shadow material (McPherren and Kuiper 2013). They found no crystallographic preferred orientation in precipitated quartz in the strain shadow, possibly a product of confined crystal growth by bounding hydrous sheets, observed as distinct wedges between similarly natured quartz (Mosher 1978; McPherren and Kuiper). As expected there is a reported increase of matrix minerals (mica, chlorite, chloritoid, feldspar and magnetite) away from the strain shadow (e.g., Mosher 1978; McPherren and Kuiper 2013). The long axis of clasts are all aligned and appear congruent with the trend of the regional fold axis, that is N-S, the result of both clast rotation and in certain area reflect plane-strain deformation (Mosher 1978; for clast rotation in a granular aggregate see Jeffrey, 1922; or Freeman, 1987; field observation). Penetrative ductile deformation is not apparent in any of the deformed clasts and has recently been affirmatively ruled out by mineralogical analysis of cobble margins (McPherren and Kuiper 2013). First recognized by Mosher (1978) there exist thin micaceous selvages along clast margins, a result of dissolution and transport of quartz, the most soluble mineral present in this system [Figure 7]. Furthermore, quartz grains inward of cobble margins were shown to lack selvages and have no history of pressure solution (McPherren and Kuiper 2013).

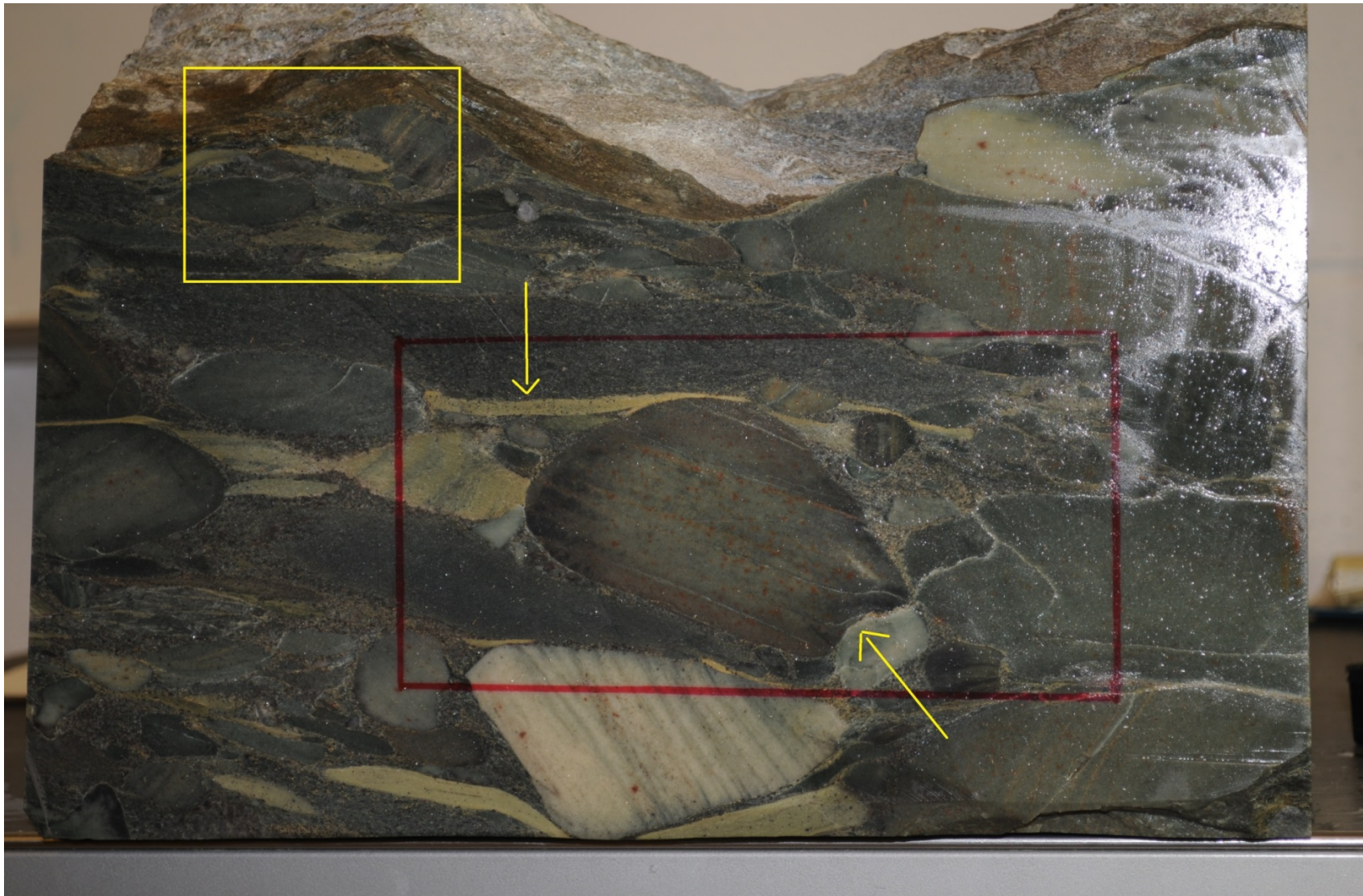


Figure 6a - XZ section of conglomerate. Arrows indicate mutual indentation (bottom) and remarkable strain (top). Yellow Box is shown enlarged on next page. Red box (4"x8" for scale)



Figure 6b - Magnetite overgrowths within cobble interiors and other pressure solution relicts. Note the varied lithology

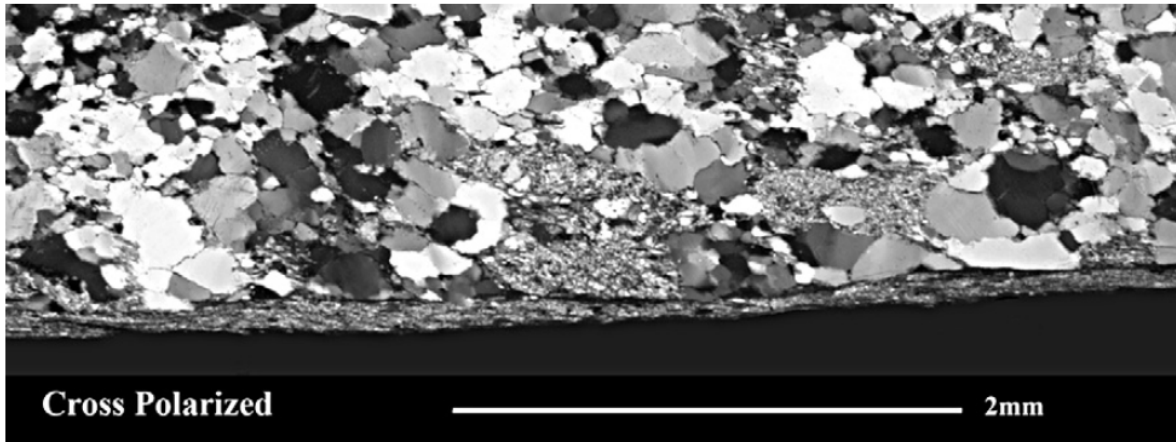


Figure 7 - Micaceous selvages present at the cobble rim, a result of quartz dissolution and transport. From McPherran and Kuiper 2013

It is thus imagined the applied stress was dissipated only in grains at the clast margins. At higher temperatures in the garnet-staurolite metamorphic zone to the west of Newport the onset of penetrative deformation [Figure 8] has produced strongly deformed clasts. Axial ratios for eight conglomerate outcrops have previously been made (Mosher 1978). Mosher produced volume loss estimates using axial ratios from three differently oriented conglomerate sections per site to produce 3d strains and using site 1 (WAR) as the initial clast shape. Volume loss calculations ranged from 24% to 66% (Mosher 1978) In her thesis Mosher discusses methods of resolving the issue of shape change and assumptions of initial shape relative to cobble reorientation relative to the regional stress (Mosher 1978; with Ramsay 1967; Dunnet 1969; Eliot 1970; Dunnet and Siddans 1971; and Mathews *et al.* 1974) Since then, the work of Freeman (1987) and others have continued the study of the evolution of passive markers, such as grains or cobbles, in a flowing system. Mosher attributes ~20% of the total volume lost during deformation of the conglomerate to intracobble shearing along cracks within cobbles. Mosher produced a combined history of metamorphic and deformational events in the conglomerate [Appendix A:1] the details of which will not be discussed in this paper. The accuracy of this M-D map may be questioned through field, hand sample, and thin section work discussed later.

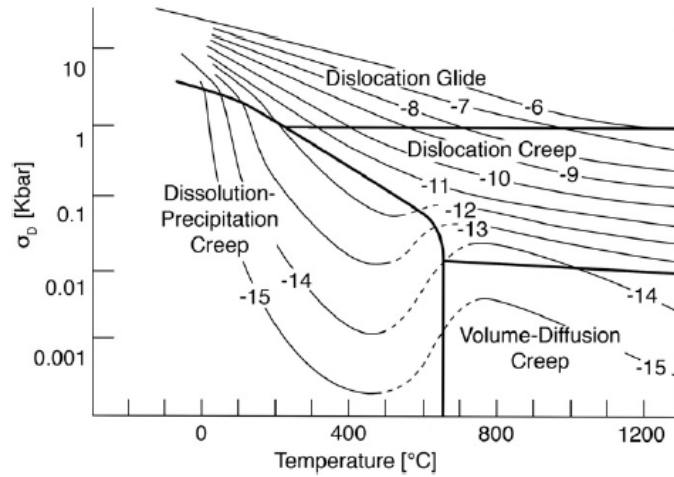


Figure 8 - PT map of deformation mechanisms. Dissolution-Precipitation Creep is equivalent to Pressure Solution. From McPherrren and Kuiper 2013 – adapted from Rutter 1976

Sites Used In This Study

11 outcrops of conglomerate spanning 10 kilometers east to west were used in this study. They are presented here from west to east. Please refer to Figure 4:

Newport & Middletown, Aquidneck Island, Rhode Island

Site 1 (WAR): Outcrop is on the western shore of the Naval base and training school. This site was Mosher’s reference undeformed conglomerate for volume loss analysis. Cobbles appear oblate

Site 2 (WEP): Outcrop is on the west side of Easton Point; the eastern extent of First Beach in Newport. There is clear interbedded Rhode Island Formation and rare quartz veins cut the horizontal surface striking southeast. Veins post date cobble deformation. Cobbles appear prolate.

Site 3 (PC): Outcrop is the Purgatory Chasm. The conglomerate here is part of a N-S striking limb that shows definite jointing roughly perpendicular to the fold axis, producing the chasm for which the site is named. Clasts appear prolate and range in size from pebbles to boulders.

Site 4 (SB): Outcrop is in the middle of Second Beach and appears to be part of the same structure as site 3 (PC). Clasts appear prolate.

Site 5 (NP): Outcrop is next to the water station at Nelson's Pond, just north of Second Beach and accessed by private driveway. Clasts appear prolate.

Site 6 (QRY): The Peckham Brother's Quarry. Exposure is abundant, including quarried wall with continuous vertical exposure of over 15 meters in many orientations, allowing for inspection of conglomerate that has not been subject to the amount of surface weathering as the other sites.

Site 7 (WLR): Conglomerate is exposed on the southeast corner of Sachuest Point Wildlife Refuge. The clasts are mixed quartzite and granite fragments, appear prolate, and few exceed 10cm in long axis dimension. This outcrop is believed to not be the Purgatory Conglomerate but the basal Pondville Conglomerate. The east side of Sachuest Point also has pre-Pennsylvanian volcanic rocks. (Quinn 1963)

Site 8 (IT): Outcrop is at the site Indian Terrace located at the end of Peckham Road in Middletown. Clasts appear prolate and jointing is significant. Mosher (1978) notes a thrust zone to the north of our study site where deformation produced oblate cobble shapes.

All Sites East of Aquidneck Island, Rhode Island

Site 9 (FOG): Conglomerate is exposed on the west shore of Fogland Point and is best observed and accessed at low tide. Clasts appear oblate and contrast the prolate clast geometries found at Indian Terrace, located to the west just across the bay.

Site 10(NA): Outcrop is behind Norm's Auto Garage, located 3363 Main Road, Tiverton, RI. Exposure is continuous for roughly 10 meters in the vertical and produces a local topographic high.

Site 11 (PPP): Outcrop is located behind Past & Present Places roughly 2 km north of Norms Autos on Main Road in Tiverton. Clasts appear roughly spheroidal and no fibrous overgrowth is observed. Conglomerate is well exposed in this area and there is a USGS Bedrock marking in the conglomerate across the street.

Methods

Shape Analysis

Volume strain data for the Purgatory conglomerate was calculated following the method of Shimamoto and Ikeda (1976); construction of a strain ellipsoid from two-dimensional analyses of at least three mutually orthogonal planes. Data was generated in the following way;

The strike and dip of a white board resting on the surface of the conglomerate were taken, aligned such that the long dimension of the white board was horizontal and strike defined as the positive x

direction. A photograph of the conglomerate with the whiteboard in this orientation was taken to ensure a fully rectified image, orient the section ellipses, and give the data a length scale.

Rectification was done piecewise; using both *Didger* and an inhouse MATLAB script. Clast margins from a rectified photo were then traced using *Didger* generating a text file containing data points defining clast margins. Tracing pebble sized clasts produced around 100 points, while large cobbles and boulders might generate over 10^3 data points. Ideally, only rocks with continuous regular boundaries were traced. The amount of clast margin inferred or extrapolated due to weathering or other factors is on the order $10^{-3}\%$ and was performed only when necessary to ensure sufficient acquisition of passive markers for Rf/ϕ analysis. The number of cobbles traced for generation of each section ellipse varied based on quality of clast identification. When possible, over 40 cobbles were traced. Section ellipse data was then entered into a program RFPSHIM, based on the Shimamoto and Ikeda method, to produce an average section ellipse for each photographed orientation. This section ellipse is defined by a long and short axis, orthogonal by definition, lying in the plane of the photograph with an apparent orientation. Three or more oriented photographs were analyzed per site. Section ellipse data was then entered into a program STRAIN3D, written by Mark Brandon, which generates a three-dimensional strain ellipsoid (using a method modified from Owens 1984). The trend, plunge, and stretch of the three principal stretch axes S_x , S_y , and S_z , are given, as well as an isotropy value for the probability that the difference in principal stretches is due to chance alone.

Modal Abundance of Fibrous Overgrowth

The modal abundance of fibrous overgrowth for each site was calculated, following Ring and Brandon (1999). This was done in a simple manner; taking the quotient of the total length of observed precipitated fibrous overgrowth in a transect and the adjusted transect length. The amount

of fibrous overgrowth was easily determined by visual inspection, and rarely did a continuous overgrowth exceed 1cm in dimension. Total transect length was adjusted to account for post-ductile strain vein and fracture development as well as any sandstone lenses that might have been crossed. For uniaxial fiber growth, the maximum stretch $S_x = 1/(1-m)$ where m is the modal fiber abundance (Ring and Brandon 1999).

Volume Loss

Volume loss estimates for each site and averaged for the conglomerate were generated by entering data from STRAIN3D into MEANDEF. MEANDEF calculates volume loss, internal rotation, and other parameters useful for strain analysis. Clast outlines served as elliptical passive markers for volume loss calculation following the method of Shimamoto and Ikeda (1976). The change in axial ratio R and alignment of clast major axes Φ by SMT deformation from an assumed random initial distribution (Φ_i, R_i) allows for volume loss estimates. Eloquently put, “The average initial ellipse represents precisely a circle centered at the origin for any distribution of the initial axial ratio R_i , if an infinite number of objects are included” (Shimamoto and Ikeda 1976). During SMT deformation of the Purgatory Conglomerate, the major axis of the clasts is assumed to have undergone no deformation (i.e., non-constant volume constrictional plane strain, $S_x=1$), preserving a dimension of the initial sphere. For volume loss calculations using MEANDEF the major stretch S_x was adjusted to account for the precipitated fibrous overgrowth, as detailed in the previous section.

Fold Axis

The fold axis for the Purgatory Conglomerate was calculated using bedding orientations from the RI state map and from measurements in the field. This was made extremely easy using Rick Allmendinger’s program *Stereonet* which calculates the fold axis and axial fold plane from poles to bedding planes.

Results

Trend, plunge, and the normalized magnitude of the three principal stretches, along with volume strain, are presented for all 11 sites [Figure 9]. The fold axis trend and plunge was found to be $192.7^\circ/013.0^\circ$. A stereonet plot of trend and plunge of outcrop S_x and of the fold axis shows strong alignment of the two for 8 of the study sites [Figure 10a]. A stereonet plot of the pole to the flattening plane and the trend and plunge of S_z for study area shows strong alignment of the strike of S_z with the normal of the flattening plane, however there is more than 30° variation in plunge, with the S_z of Site 7 (II) inclined more than 50° relative to most study sites [Figure 10b]. A Flinn diagram comparing R_{xy} to R_{yz} gives an idea of the general shape – prolate (cigar-shaped) above the plane strain line and oblate (pancake-shaped) below. A Nadai type diagram plots R_{xz} against the deviatoric stretch S'_y , given by $S'_y = S_y/S_v^{1/3}$. These can be found in the Appendix (Appendix A:2). Calculating deviatoric stretch for this study is a useful way to determine how deformation was distributed across the two minor axes, as S_x was assumed to undergo no appreciable stretch during deformation. The two figures complement each other well and demonstrate the distribution of clast geometries across the basin.

Discussion

Regional Variation in Volume Loss and Ellipsoid Geometry

Average volume loss for the 11 sites is 82.6%, increasing towards the interior of the study area. 7 of the study sites have the major stretch S_x oriented within 8° of trend and 10° of plunge, 6 of which have distinct prolate geometries (Sites 2, 3, 4, 5, 6, 8). Orientations of S_y values for these 6 sites are similarly correlated with the regional S_y , all within 11° of trend and varying more in plunge.

Site Number	Site Name	Trend S_x	Plunge S_x	S_x	Trend S_y	Plunge S_y	S_y	R_{yx}	Trend S_z	Plunge S_z	S_z	R_{zx}	S_v
1	WC	61	11	1.02	326	26	0.816	0.8	173	62	0.466	0.45714286	0.37
2	WEP	192	3	1.009	101	19	0.448	0.44385027	289	71	0.351	0.34759358	0.16
3	PC	188	5	1.0056	95	30	0.366	0.36407767	285	59	0.317	0.31553398	0.12
4	SB	4	1	1.007	94	21	0.281	0.27888446	270	69	0.229	0.22709163	0.06
5	NP	184	11	1.007	280	30	0.354	0.35121951	75	57	0.334	0.33170732	0.12
6	QRY	192	10	1.0066	289	36	0.419	0.41578947	89	53	0.355	0.35263158	0.15
7	WLR	128	37	1.0177	33	7	0.607	0.59659091	294	52	0.312	0.30681818	0.19
8	IT	185	8	1.014	61	76	0.376	0.37128713	277	12	0.331	0.32673267	0.12
9	FOG	195	5	1.008	104	16	0.616	0.61081081	303	74	0.262	0.25945946	0.16
10	NA	29	3	1.0011	120	20	0.649	0.64828588	291	70	0.395	0.39456597	0.26
11	PP	58	5	1	148	7	0.821	0.82051282	292	82	0.761	0.76068376	0.62
Average^a		189.9	4.3	0.922	098.3	20.2	0.504		291.3	69.4	0.374		0.174

Figure 9 – Results of MEANDEF and STRAIN3D. S_x , S_y , and S_z are the principal stretches normalized such that $S_x=1$ + the modal abundance of fibrous overgrowth. See text for discussion.

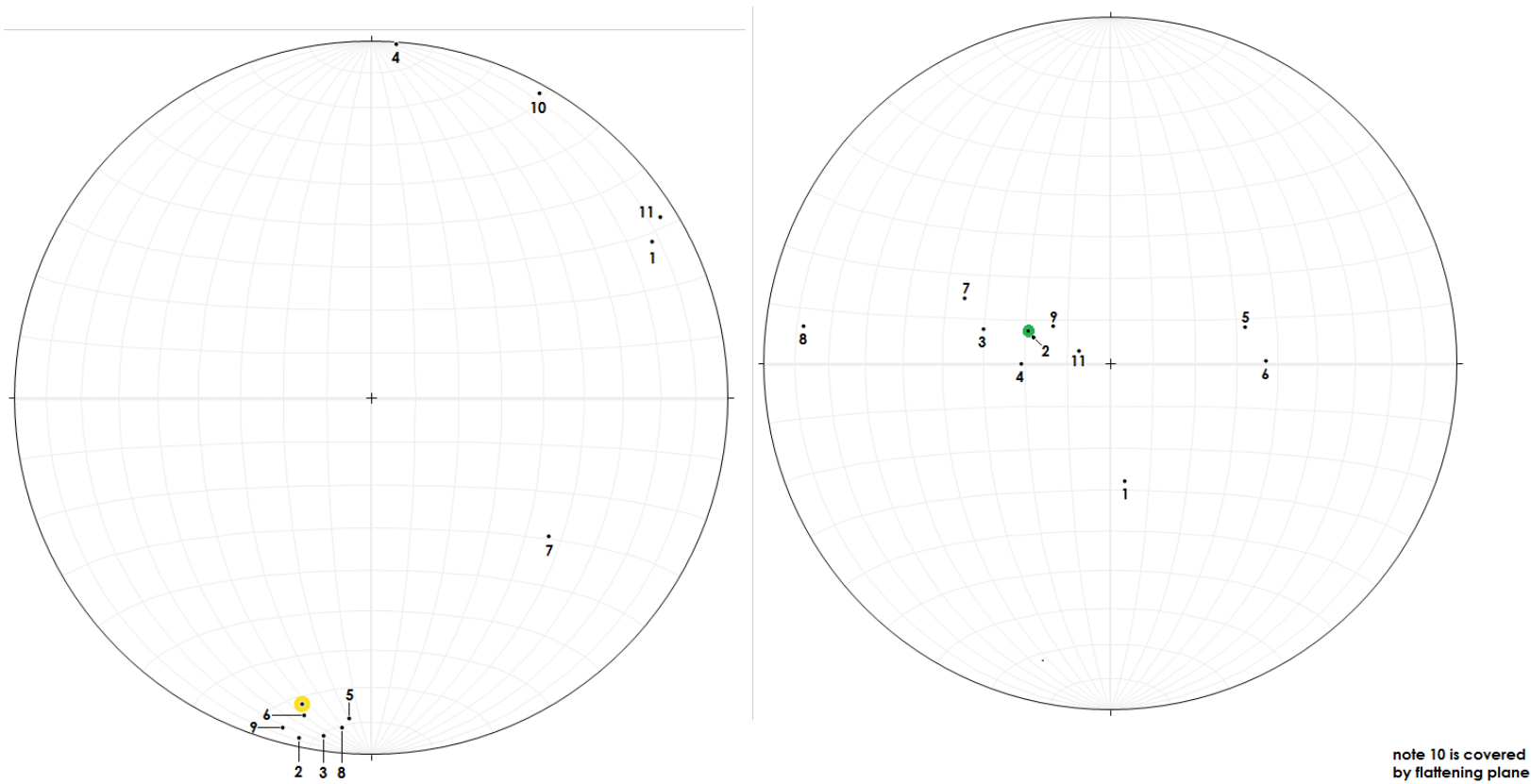


Figure 10a – Stereonet projection of the regional fold axis (yellow marker) with the S_x trend and plunge of the study area.

Figure 10b – Stereonet projection of the pole to the flattening plane (green marker) with the S_z trend and plunge of the study area.

Average volume loss across these 6 sites is 88.8% and all have an increase in S_x by fibrous overgrowth of $\leq 1\%$. The Y and Z axes of these prolate exposures are less well aligned yet remain in agreement the distribution of stresses inferred from the orientation of the fold axis; that is roughly east-west. The continuity of S_x orientation across sites 4 and 5 is supported by their proximity and it is inferred the two exposures are of the same portion of the folded conglomerate layer.

Site 9 (FOG) is the only site with distinct oblate geometry and is the 7th site with alignment of S_x to the regional fold axis. R_{yz} , not presented in Figure 9, is greater than 2, and R_{yx} is 0.6. In nature the clasts of Fogland Point appear flattened and pancake-shaped, however $S_x > S_y > S_z$ and thus clasts have been flattened into football shaped pancakes. This result indicates the flattening associated with deformation of site (9) was accompanied by the regionally defined east-west maximum stress σ_1 . Volume loss in the clasts of Fogland Point was 84%, suggesting reorientation of stresses producing oblate geometries did not effect rate of SMT. It is also possible the clasts at this location had depositionally developed preferred orientations prior to deformation.

The easternmost sites (10) and (11) show a decrease in total volume loss as well as ellipsoid anisotropy. Clasts of the conglomerate at Norms Autos have lost 74% of their volume and S_x trends 17 degrees to the west of the fold axis. Conglomerate exposed behind Past and Present Places, the north eastern extent of the present study area, has lost 38% of its volume, significantly less than the other 10 sites. The major stretch S_x is oriented to the northeast ($058^\circ/05^\circ$) and there is no observable fibrous overgrowth on the margins of the clasts. Volume strain deformation is here observed to be fairly isotropic. It is interesting to note the alignment of the flattening direction, S_z , between sites 10 and 11 ($291/70$ and $292/82$ respectively) and the regional average ($291.3/69.4$), again reflecting the regional EW compressive folding.

The westernmost site (WAR:1) has experienced less volume loss (63%) than the interior sites and the major and intermediate stretches S_x ($061^\circ/11$) and S_y ($326^\circ/26^\circ$) are aligned with that of the easternmost site, Past and Present Places. The minor stretch S_z of site 1 is poorly correlated to that of site (11), both in magnitude (0.466 vs. 0.761) and in orientation ($173^\circ/62^\circ$ vs $292^\circ/82^\circ$).

Site 7, the Wildlife Refuge, has strain data unlike all other sites except for total volume loss (81%). The major stretch axis S_x is oriented $\sim 62^\circ$ east of the fold axis and plunges 37° below horizontal. Clast geometry is somewhat similar to that of Fogland Point across the bay, however poor alignment of principal axes makes correlation difficult. Furthermore, the conglomerate studied at the Wildlife Refuge is quite granitic and believed to be a part of the basal Pondville Conglomerate. If that is the case, there are at least three reasonable hypotheses for the development of a unique strain ellipsoid;

- (1) The Pondville Conglomerate was subject to differently oriented stresses, or
- (2) Exhumation did not maintain orientation of the deformation.
- (3) Clasts had a depositionally developed preferred orientation

The second explanation is plausible, considering lack of exposure of the Pondville in the region. Perhaps the exposure of interest (7) is a faulted block of the older conglomerate exhumed significantly after the pressure solution deformation event, changing the orientation of principal axes from their initial position to what is observed now. If clasts of this exposure were oriented similar to those of Fogland Point prior to exhumation, the rotation indicates motion around the minor axis accompanied by a slight vergence of S_z to the horizontal (FOG $S_z = 303^\circ/74$, WLR $S_z = 294^\circ/52$). S_z of WLR is slightly less than that of FOG, which might support reorientation of S_z during deformation away from the pole to the flattening plane. This outcrop and strain data may be useful in a more detailed tectonic reconstruction of the deformation of the Purgatory Conglomerate.

The strong similarity shown in the prolate clasts of sites 2,3,4,5,6, and 8 suggest at least one hypothesis for the apparent constriction;

- (1) Rotation of the clasts or the bulk rock around the fold axis, preserving S_x and distributing σ_1 throughout the YZ plane.

This would be accomplished if the exposures were all deformed in the hinge or kink of regional folds during pressure solution mass transfer, resulting in both greater surface area of the solid that is stressed and rotation of clasts. Mosher (1978) noted the presence of many north-south striking normal faults developed throughout the basin that developed without any strike-slip motion. If these faults were active during deformation it is understood that stresses on clasts in proximity to these faults would be greatly and redistributed. Mosher (1978) discovered a thrust zone just to the north of site (8) which she argued is associated with oblate clast shapes and the precipitation of sulfide metals in close proximity to the active fault (~30 feet). This area of intense deformation is continuous with the surrounding prolate clasts of Indian Terrace, and it is thus assumed the north-south faults in these areas were not too active, as exposures of the above have not been found otherwise.

Clasts of site (11) do not appear at first glance to be of significantly different size than the other 10 sites, however the conglomerate has varying clast sizes between and within outcrops. Until more detailed inspection of clast size distribution is made the disparity in volume loss remains an intriguing result. An issue of significant relevance in quantifying the accuracy of the presented volume loss data is the potential for clasts to undergo significant rotation of their principal stretch axes out of alignment with the regional fold axis by rotation of the entire clast. This would result in reorientation of stresses such that the long axis would no longer be oriented normal to the perceived east-west plane of constriction. Any stretch and reorientation of S_x obviously skews the calculated

volume loss estimates due to failure of the condition that the initial S_x is preserved through deformation. Furthermore, a scenario where deforming ellipsoidal clasts rotate under a constant stress field would likely diminish pronounced features producing spheroidal roundstones

(see Freeman 1987a, b and sources therein). No fibrous overgrowth was observed at this site, the cause of which remains unclear. Differences in the physiochemical nature of the fluid involved in deformation across the region may have influenced this, as would increased rotation of clasts. The fibrous overgrowths are unanimously observed on the long axis terminations at the other sites and show no rotational fabric themselves. If more rotation of the long axis occurred at site 11 during deformation one could envision either continuous dissolution of previously formed strain shadows, or lack of overgrowth precipitation altogether.

If rotation of clasts irrespective of the regional fold axis at site PPP is responsible for their relatively isotropic geometry, the same may be said for the easternmost outcrop WAR. WAR experienced the second least amount of volume loss (63%), however does have an apparent flattening ($S_y=0.816$, $S_z=0.466$, $173^\circ/62^\circ$). Furthermore, fibrous overgrowth is observed, immediately raising questions of the relation between the eastern and western margins of the basin. It should be noted that although clasts at Norm's Autos do have fibrous overgrowths their modal abundance is almost an order of magnitude less than sites to the west. Resolving the issue of clast rotation during deformation appears quite important to better quantify the pressure solution mass transfer history of the deformed Purgatory Conglomerate.

Another consideration is that of volume loss accommodated by intracobble shear fracture. Dissolution and sliding of cobble pieces along fractures would contribute to volume loss. Mosher (1978) estimates this mechanism was responsible for about 15-20% of the observed volume strain. Recent observation challenges this hypothesis. Intracobble fracture is recognized however is not

observed in the majority of cobbles. Furthermore, fracture appears to have offset the mature cobble shapes indicated by minimal, if any, cobble margin offset. Outcrop scale fracture and post metamorphic vein development is observed, however is not significant for any outcrop. Line transects across the faces of Quarry Rock, similar to calculations made for the modal abundance of fiber, might better quantify the prevalence of intracobble fracture.

Fluid Physiochemistry

It is apparent that the aqueous fluid involved in the solution mass transfer studied here had to carry an impressive solute load. It is generally accepted that a number of geological phenomena can produce variation in fluid properties allowing such transport capacity. To name a few:

- (1) Fluid traveling up-gradient in temperature [Figure 3]
- (2) Fluid increasing in pH [Figure 11]
- (3) Large Darcian fluxes allow for large solute transport

A fluid can increase in temperature in a number of ways in geological systems, perhaps by moving down in the crust heated by the regional geothermal gradient. The lengthscale to which silica was transported away from the conglomerate is an important question; locally it is reasonable to consider intrusion of the Narragansett Pier Granite as a possible heat source to drive fluid flow and silica transport. Deformed conglomerate found under the Jamestown Island Bridge is at a higher grade. The clasts are internally deformed, presumably due to dislocation glide mechanism, which would have been more active at higher temperatures. The deviatoric strain is large but the volume strain is unknown.[Figure 8]. It is reported that conglomerate exposure to the west and north of Jamestown Island has undergone variable shear and flattening deformation (Shaler 1989) such that

variation of temperature across the study site may produce geologically significant variation in strain rate, even across the 11 sites presented here. A block of deformed conglomerate sampled underneath the Jamestown Bridge, where staurolite is present in the interbedded shale and garnet pervades the conglomerate, will assist in future determination of the more penetrative deformations associated with the evolution of the Narragansett Basin.

The solubility of quartz with respect to pH has been well studied [Figure 11] (see Tang and Su-Fen 1980; Knauss and Wolery, 1988 for low T experiments; Rimstidt, 1997) and increases significantly when the pH of the aqueous rises above that of neutral solution (pH = 7.0).

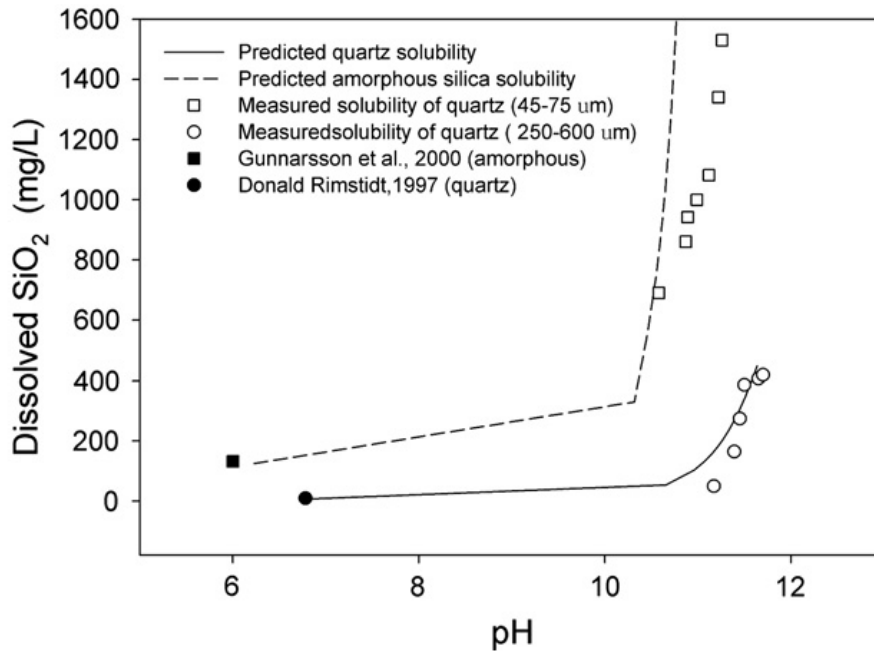


Figure 11 - Silica solubility with pH, determined using NH₃. From Wang et al 2011

It has similarly been shown that hydrolysis of silica at low temperatures (70°C) is pH independent only in very acidic environments, switching to pH dependent solubility in solutions that are weakly acidic (pH ~ 6) (Knauss and Wolery, 1988; Siever 1962). Lab experiment shows that an increase in

pH from weakly acidic (pH = 6) to basic (pH=11.8) produces a dissolution rate almost four orders of magnitude greater (Knauss and Wolery, 1988). There are few natural processes that can produce alkaline fluids: (1) a rise in pH due to anaerobic methane oxidation coupled to sulfate reduction, (2) extensive calcite dissolution, and (3) a late stage fluid evolved from an ultramafic intrusion. (Meister et al, 2011; Salvi and Jones, 2006). Our study of the Purgatory Conglomerate indicates a few possible sources of alkalinity. Intrusion of the Narragansett Pier Granite to the southwest, responsible for the observed metamorphic zoning, might have significantly altered fluid alkalinity during convection. Sulfide mineralization at various conglomerate outcrops might support sulfate saturation at depth. In at least one site intense sulfide mineralization accompanies uncharacteristic shape change (Site 8 IT; Mosher, 1978) The sulfide metals pyrite appears in some hand samples at both site 8 (IT) and site 9 (FOG). Field evidence suggests the conglomerate is in stratigraphic sequence with not only lithic greywacke sandstone but organic-rich coaly shale (Shaler, 1899). Complexation and ion exchange between an aqueous fluid and organic species in diagenetic or low metamorphic grade systems has the potential to increase mobility of silica cations in solution (e.g., Bennet and Siegel, 1987). In their study Bennet and Siegel aimed to determine the relationship between silica solubility and organic carbon concentration, and report a linear relationship between the two. For this project, little carbonate is observed in the matrix, within strain shadows or at cobble margins, nor in the nearby sandstone layers or in post metamorphic quartz veinages. The presence of magnetite overgrowths penetrating clast interiors, strain shadows, and matrix – seen in thin section and hand sample of preserved conglomerate – might suggest episodic mixing of an anoxic convective fluid saturated in ferrous iron (Fe^{3+}) with oxygenated meteoric water resulting in ubiquitous magnetite precipitation. The relationship between sulfur and quartz solubility is poorly studied, however some relationships can be estimated. It is expected than an increase in sulfur activity in an aqueous solution decreases the pH due to speciation of sulfuric acid. Although this would traditionally drive silica solubility

down, it has been noted for quite some time that increase in activity of strong ionic species in solution increases solubility – most likely due to complexation of ionic silica into molecular species to be subsequently transported away from sites of dissolution (e.g., USGS 1977). A detailed explanation of the nature of geochemical variation in different fluid systems is presented in a 1977 USGS paper (USGS 1050), in which it is noted that “... organic acid anions contribute significantly to the measured alkalinities”. It is thus understood that fluid infiltration through organic rich layers will introduce a number of chemical species to the fluid solute activity profile. While these species may produce acidic solutions in certain systems it is here perceived the presence of coaly shale layers near the conglomerate act as sources of organic anions, increasing silica solubility.

If pore water velocities are significant during deformation of the Purgatory Conglomerate the nature of grain boundary-pore fluid interactions are altered. A thinning of the boundary film due to the no-slip condition along fluid-grain contacts effectively compresses the solute concentration gradient normal to the grain surface. This results in the solute concentration of the advecting pore water, assumed to be quite low, being distributed in close proximity to the boundary fluid. This would in theory result in solute ‘scavenging’ from the grain boundary fluid film. If the solute gradient between the grain boundary film and the pore fluid is large it is expected solute would leave the grain boundary fluid once diffusion has brought solute to the pore space, away from the stressed solid interface.

Conclusions

Volume loss estimates for the Purgatory Conglomerate indicate significant pressure solution mass transfer deformation. Data accurately represent the 3d geometries of the clasts of the conglomerate. Prolate cobbles interior to the study area have correlated prolate geometries, have undergone the greatest volume loss, and are undoubtedly the result of constriction in an east-west YZ plane. Rotation of the cobble long axis after initial alignment with the fold axis is perceived not to occur. Strain ellipsoids produced for the marginal sites tell a different story – less apparent volume loss, more oblate or triaxial geometries, and curiously aligned minor stretches. The easternmost site has undergone the most isotropic volume loss and lacks visible fibrous overgrowths, posing new questions about the structural and hydrological evolution of the conglomerate.

A detailed discussion of the water-rock interaction resulting in significant apparent volume loss has been included. A number of naturally varying parameters might have influenced the solubility and transport of silica during pressure solution mass transfer, and it is likely a combination of dynamic changes in temperature, fluid alkalinity and chemistry, and physical flow that produced the ability to transport the large solute load assumed.

Work will continue to focus on the mass transport characteristics of the deformation of the Purgatory Conglomerate. Oxygen isotope analysis of the cobbles (see appendix), strain shadows, and matrix will help in understanding some of the illustrated hydrological conditions. Thin section analysis will shed light on the overprinting of metamorphic minerals and their subsequent solution, as well as the nature of selvage formation and healing of fractures. Fluid inclusion analysis of strain shadows could be immensely useful in reconstructing P-T-X conditions of the solvent.

Acknowledgements

I would like to thank professor Mark Brandon for his guidance on this project and throughout my time at Yale. Chris Thissen has educated me in many ways during the project and has been my partner in many day trips to RI. Professors Zhengrong Wang and Danny Rye have been quite helpful in discussion of general geology and a geochemical model for water-rock interaction. Bill and Chris in the Rock Lab – you guys were tremendous in getting me acquainted with using the machines in the shop and cutting the large blocks. Many Thanks! I would similarly like to thank Julien Peckham of Peckham Brothers Quarry in Middletown Rhode Island for providing samples, allowing the department field trip, and historical discussion. A big thanks to all other locals who provided information on possible conglomerate outcrop. The Yale College Deans Research Fellowship and Yale Environmental Summer Fellowship provided funding for this project.

Works Cited

- Adams, F. D., & Coker, E. G. (1910). "An experimental investigation into the flow of rocks; the flow of marble." *American Journal of Science*, (174), 465-487.
- Bennett, P., and D. I. Siegel. (1987) "Increased solubility of quartz in water due to complexing by organic compounds." *Nature* 326, 684-686.
- Bennett, P. C., Melcer, M. E., Siegel, D. I., & Hassett, J. P. (1988). "The dissolution of quartz in dilute aqueous solutions of organic acids at 25 C." *Geochimica et Cosmochimica Acta*, 52(6), 1521-1530.
- Brandon, M. T., Cowan, D. S., & Feehan, J. G. (1994). "Fault-zone structures and solution-mass-transfer cleavage in Late Cretaceous nappes, San Juan Islands, Washington." In *Geologic field trips in the Pacific Northwest: Geological Society of America annual meeting*, Seattle, University of Washington, Department of Geological Sciences, p. 2L-1–2L-19.
- Coble, R. L. (1963). "A model for boundary diffusion controlled creep in polycrystalline materials." *Journal of Applied Physics*, 34, 1679.
- b. Paladino, A. E., & Coble, R. L. (1963). "Effect Of Grain Boundaries on Diffusion-Controlled Processes in Aluminum Oxide." *Journal of the American Ceramic Society*, 46(3), 133-136.
- c. Coble, R. L., & Guerard, Y. H. (1963). Creep of polycrystalline aluminum oxide. *Journal of the American Ceramic Society*, 46(7), 353-354.
- De Boer, R. B., Nagtegaal, P. J. C., & Duyvis, E. M. (1977). "Pressure solution experiments on quartz sand." *Geochimica et Cosmochimica Acta*, 41(2), 257-264.
- Dunnet, D. (1969). "A technique of finite strain analysis using elliptical particles." *Tectonophysics*, 7(2), 117-136.
- Dunnet, D., & Siddans, A. W. B. (1971). "Non-random sedimentary fabrics and their modification by strain." *Tectonophysics*, 12(4), 307-325.

- De Paor, D. G. (1980). "Some limitations of the R_f/φ technique of strain analysis." *Tectonophysics*, 64(1), T29-T31.
- Durney, D. W. (1976). "Pressure-solution and crystallization deformation". *Philosophical Transactions of the Royal Society of London. Series A, Mathematical and Physical Sciences*, 283(1312), 229-240.
- Elias, B. P., & Hajash, A. (1992). "Changes in quartz solubility and porosity due to effective stress: An experimental investigation of pressure solution." *Geology*, 20(5), 451-454.
- Elliott, D. (1970). "Determination of finite strain and initial shape from deformed elliptical objects." *Geological Society of America Bulletin*, 81(8), 2221-2236. Eliot 1970
- Fournier, R. O., & Potter, R. W. (1982). "An equation correlating the solubility of quartz in water from 25 to 900 C at pressures up to 10,000 bars." *Geochimica et Cosmochimica Acta*, 46(10), 1969-1973.
- Freeman, B., & Lisle, R. J. (1987). "The relationship between tectonic strain and the three-dimensional shape fabrics of pebbles in deformed conglomerates." *Journal of the Geological Society*, 144(4), 635-639.
- b. Freeman, B. (1987). "The behaviour of deformable ellipsoidal particles in three-dimensional slow flows: implications for geological strain analysis." *Tectonophysics*, 132(4), 297-309.
- Gibbs, J. W. (1878). "On the equilibrium of heterogeneous substances." Connecticut Academy of Arts and Sciences.
- Gibbs, J. W. (1906). "Thermodynamics." Longmans, Green, and Company.
- Jeffery, G. B., (1922). "The motion of ellipsoidal particles immersed in a viscous fluid." *Proceedings of the Royal Society of London*, 0A102, 161-179
- Kay, M. (1951) "North American geosynclines." *Geol. Soc. Amer. Mem.*, 48, 143p
- Knauss, K. G., & Wolery, T. J. (1988). "The dissolution kinetics of quartz as a function of pH and time at 70 C." *Geochimica et Cosmochimica Acta*, 52(1), 43-53
- Krauskopf, K. B. (1956). "Dissolution and precipitation of silica at low temperatures." *Geochimica et Cosmochimica Acta*, 10(1), 1-26.
- Lahee, F. H. (1912). "Relations of the degree of metamorphism to geological structure and to acid igneous intrusion in the Narragansett Basin, Rhode Island". *American Journal of Science*, (197), 447-469.
- Lehner, F. K. (1995). "A model for intergranular pressure solution in open systems." *Tectonophysics* 245(3) 153-170
- Matthews, P.E., Bond, R.A.B. and Van der Berg, J.J., (1974)." An algebraic method of strain analysis using elliptical markers." *Tectonophysics*, 24(1/2): 31-67. Mathews et al 1974
- McPherrren, E. D., & Kuiper, Y. D. (2013). "The Effects of Dissolution-Precipitation Creep on Quartz Fabrics within the Purgatory Conglomerate, Rhode Island." *Journal of Structural Geology*.

- Meister, P., Gutjahr, M., Frank, M., Bernasconi, S. M., Vasconcelos, C., & McKenzie, J. A. (2011) "Dolomite formation within the methanogenic zone induced by tectonically driven fluids in the Peru accretionary prism." *Geology*, v. 39; no. 6. P. 563-566
- Mosher, S. (1976). "Pressure solution as a deformation mechanism in Pennsylvanian conglomerates from Rhode Island." *The Journal of Geology*, 355-363.
- Mosher, S. (1978). "Pressure solution as a deformation mechanism in the Purgatory Conglomerate." (Doctoral dissertation, University of Illinois at Urbana-Champaign.).
- Mosher, S. (1981). "Pressure solution deformation of the Purgatory Conglomerate from Rhode Island." *The Journal of Geology*, 37-55.
- Mosher, S. (1983). "Kinematic history of the Narragansett Basin, Massachusetts and Rhode Island: Constraints on late Paleozoic plate reconstructions." *Tectonics*, 2(4), 327-344.
- Mosher, S., & Rast, N. (1984). "The deformation and metamorphism of Carboniferous rocks in Maritime Canada and New England." *Geological Society, London, Special Publications*, 14(1), 233-243.
- Mosher, S. (1987). "Pressure-solution deformation of the Purgatory Conglomerate, Rhode Island (USA): Quantification of Volume change, real strains and sedimentary shape factor." *Journal of structural geology*, 9(2), 221-232.
- Owens, W. H. (1984). "The calculation of a best-fit ellipsoid from elliptical sections on arbitrarily orientated planes." *Journal of Structural Geology*, 6(5), 571-578
- Paterson, M. S. (1973). Nonhydrostatic thermodynamics and its geologic applications. *Reviews of Geophysics*, 11(2), 355-389.
- Posamentier, H. W., & Vail, P. R. (1988). "Eustatic controls on clastic deposition II—sequence and systems tract models."
- Reck, B. H., & Mosher, S. (1988). "Timing of intrusion of the Narragansett Pier Granite relative to deformation in the southwestern Narragansett Basin, Rhode Island." *The Journal of Geology*, 677-692.
- Rimstidt, J. D. (1997). "Quartz solubility at low temperatures." *Geochimica et Cosmochimica Acta*, 61(13), 2553-2558.
- Ring, U., & Brandon, M. (1999). "Ductile deformation and mass loss in the Franciscan Subduction Complex: implications for exhumation processes in accretionary wedges." In U. Ring, M. Brandon, G. Lister, & S. Willett (Eds.), *Exhumation processes: Normal faulting, ductile flow, and erosion* (pp. 55–86). Geological Society of London.
- Ring, U., Brandon, M. T., & Ramthun, A. (2001). "Solution-mass-transfer deformation adjacent to the Glarus Thrust, with implications for the tectonic evolution of the Alpine wedge in eastern Switzerland." *Journal of Structural Geology*, 23(10), 1491-1505.
- Ramsay, J. G. (1967) "Folding and Fracturing of Rocks" McGraw Hill, New York, N.Y. 568 pp.

- Rutter, E. H., & Elliott, D. (1976). "The kinetics of rock deformation by pressure solution [and Discussion]." *Philosophical Transactions of the Royal Society of London. Series A, Mathematical and Physical Sciences*, 283(1312), 203-219.
- Rutter, E. H. (1983). "Pressure solution in nature, theory and experiment." *Journal of the Geological Society*, 140(5), 725-740.
- Salvi, S., & Williams-Jones, A. E. (2006) "Alteration, HFSE mineralization and hydrocarbon formation in peralkaline igneous systems: Insights from the Strange Lake Pluton, Canada" *Lithos* 91, p. 19-34
- Shaler, N. S., Woodworth, J. B., & Foerste, A. F. (1899). "Geology of the Narragansett basin" (Vol. 33). Govt. print. off.
- Shimamoto, T., & Ikeda, Y. (1976). "A simple algebraic method for strain estimation from deformed ellipsoidal objects. 1. Basic theory." *Tectonophysics*, 36(4), 315-337.
- Siever, R. (1962). "Silica solubility, 0-200 C., and the diagenesis of siliceous sediments." *The Journal of Geology*, 127-150.
- Skehan, S. J., D. P. Murray, J. C. Hepburn, M.P. Billings, P. C. Lyons, and R. G. Doyle (1979) The Mississippian and Pennsylvanian (Carboniferous) Systems in the United States-Massachusetts, Rhode Island, and Maine, U.S. Geol. Surv. Prof. Pap., 1110A, 30 pp.,
- b. Skehan, S. J., and D. P. Murray, (1979) Geology of the Narragansett Basin, southeastern Massachusetts and Rhode Island, in Carboniferous Basins of Southeastern New England, edited by B. Cameron, pp. 7-35, American Geological Institute, Falls Church, Virginia
- Sorby, H. C. (1863). "The Bakerian lecture: On the direct correlation of mechanical and chemical forces." *Proceedings of the Royal Society of London*, 12, 538-550.
- Sorby, H. C. (1865). "On Impressed Limestone Pebbles: As Illustrating a New Principle in Chemical Geology: a Paper Read Before the Members of the Geological and Polytechnic Society on the West-Riding of Yorkshire," at *Sheffield*, Nov. 22nd, 1865. Edward Baines and Sons.
- Tada, R., & Siever, R. (1989). "Pressure solution during diagenesis." *Annual Review of Earth and Planetary Sciences*, 17, 89.
- Towe, K. M. (1959). "Petrology and source of sediments in the Narragansett Basin of Rhode Island and Massachusetts." *Journal of Sedimentary Research*, 29(4).
- USGS (1977) Publication 1050. US Govt. Print office
- Walcott, C. D. (1899). Pre-Cambrian fossiliferous formations.
- Xi Wang, Qiyuan Chen, Huiping Hu, Zhoulan Yin (2011) "Solubility and dissolution kinetics of quartz in NH₃-H₂O system at 25°C" *Hydrometallurgy*, Volume 107, Issues 1-2,
- Weyl, P. K. (1958). "The solution kinetics of calcite." *The Journal of Geology*, 163-176.

Weyl, P. K. (1959). "Pressure solution and the force of crystallization: A phenomenological theory." *Journal of Geophysical Research*, 64(11), 2001-2025.

Appendix A:1

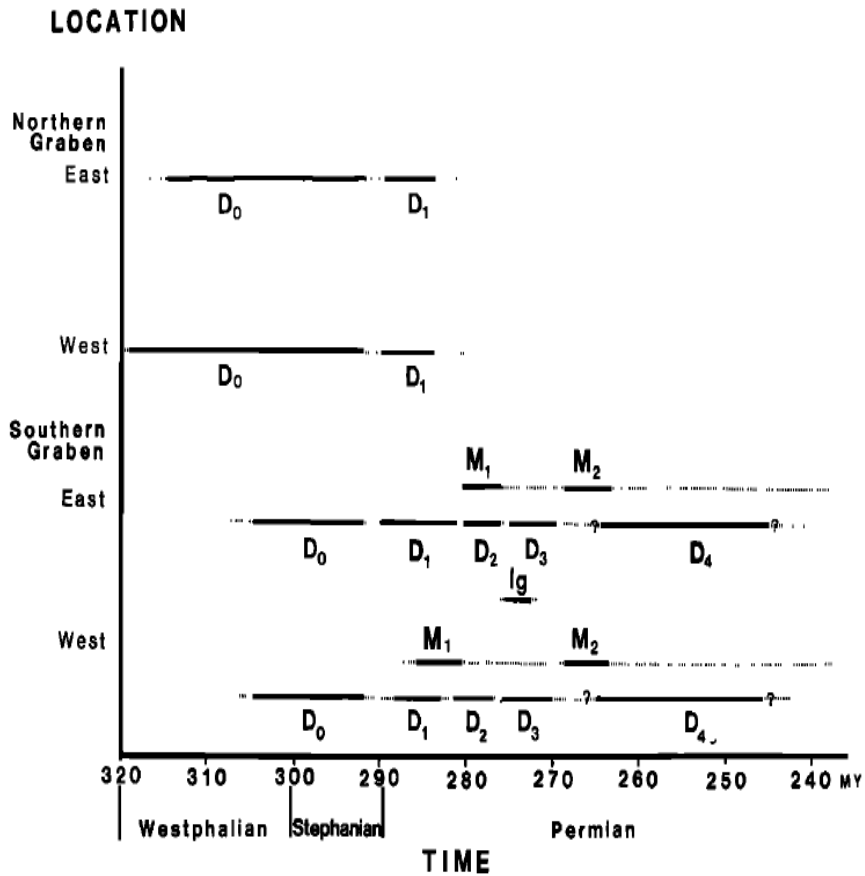
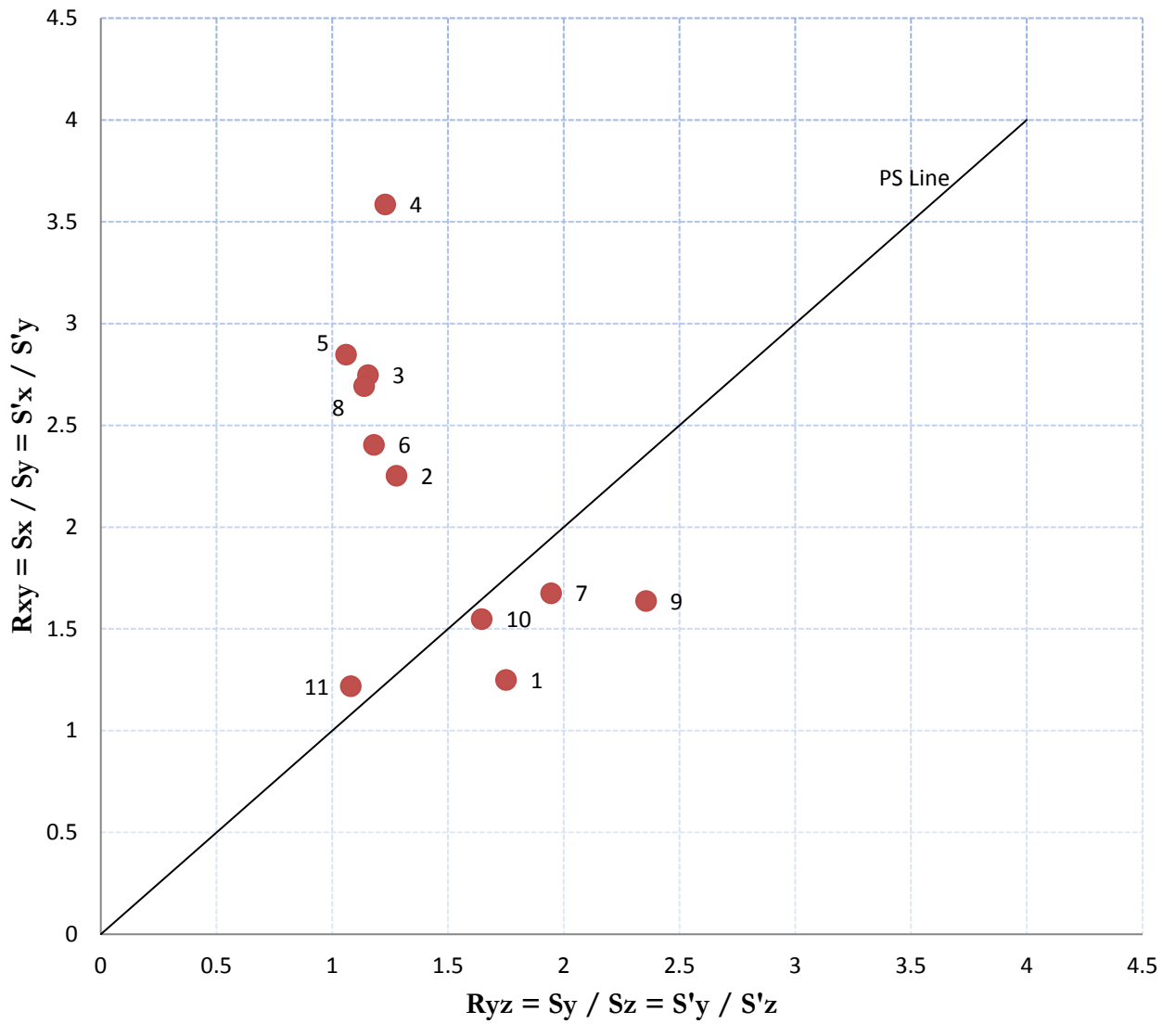


Fig. 7. Plot of location versus timing for basin formation (D₀), deformation (D), metamorphism (M), and igneous intrusion (Ig) in the northern and southern grabens of the Narragansett Basin complex. European stages for Pennsylvanian period are shown; absolute ages for stage and period boundaries are after Bouroz [1978].

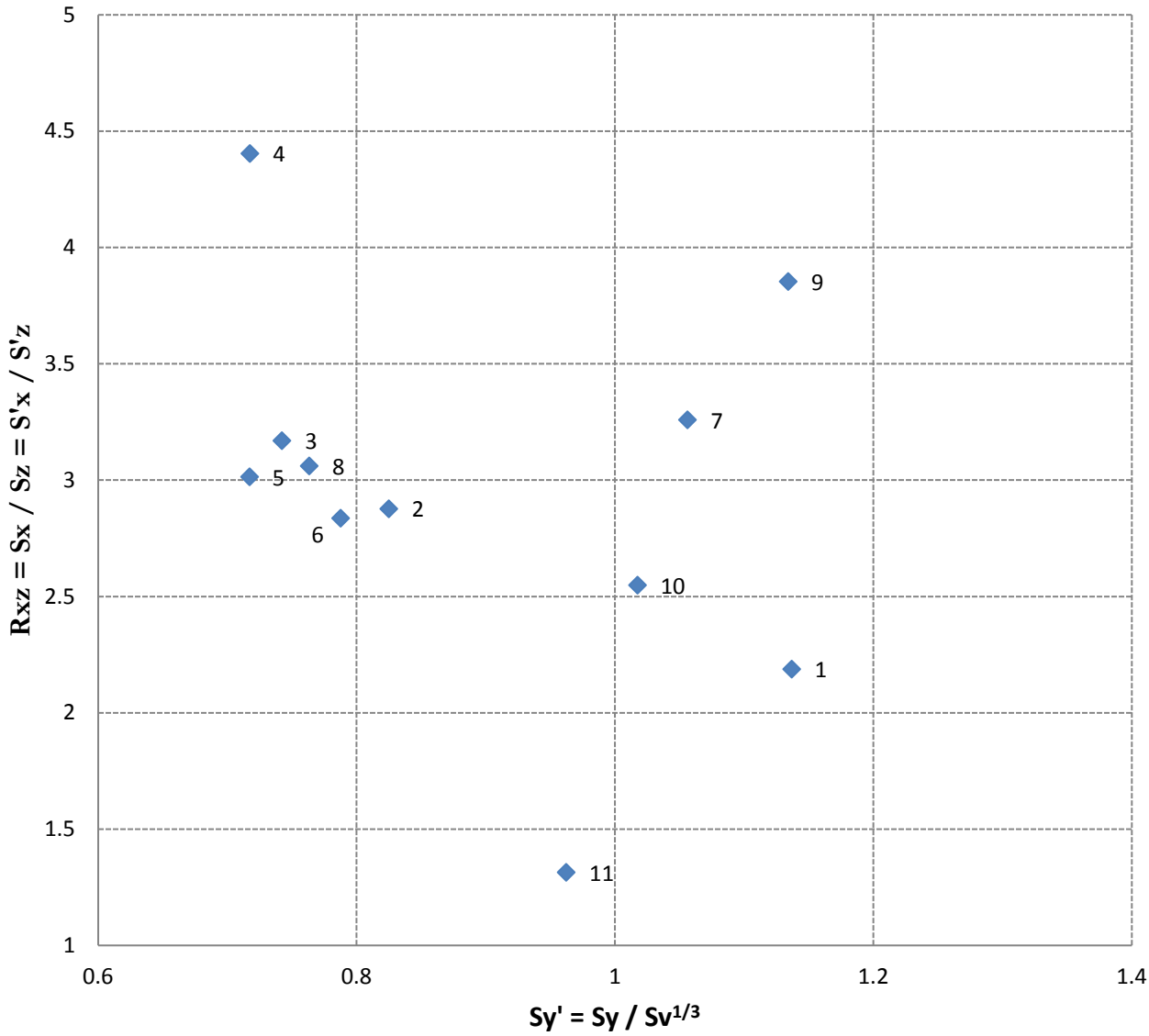
Appendix A:1 As in Mosher 1983

Flinn Diagram



A:2 Flinn Diagram. Plot of R_{xy} against R_{yz} , with a plot of the apparent plane strain line

Nadai Type



A:2 NAdai Type Diagram; a comparison of equally distributed stretch (Sy') vs apparent (R_{xx})